

## NO<sub>2</sub> adsorption on Grafoil between 297 and 12 K

R. Moreh and Y. Finkelstein

*Physics Department, Ben-Gurion University of the Negev, Beer-Sheva, Israel  
and Physics Department, Nuclear Research Center-Negev, Beer-Sheva, Israel*

H. Shechter

*Solid State Institute and Physics Department, Technion, Haifa, Israel 32000*

(Received 6 December 1995)

The NO<sub>2</sub> adsorption on Grafoil was studied using the nuclear resonance photon scattering technique. By measuring the scattering cross section of the 6324-keV  $\gamma$  line from <sup>15</sup>N, it was possible to determine beyond any doubt that NO<sub>2</sub> is adsorbed as a dimer, N<sub>2</sub>O<sub>4</sub>, on graphite. The scattered intensity ratio from the adsorbing Grafoil sample with the beam parallel and perpendicular to the graphite planes was also measured as a function of  $T$ . This yielded the tilt angle of the N<sub>2</sub>O<sub>4</sub> molecular plane which was found to be normal to the graphite planes with the N=N bond normal to the same planes. This tilt angle seems to be considerably stable between 12 and 300 K. [S0163-1829(96)01120-4]

### I. INTRODUCTION

It is well known by now that the nuclear resonance photon scattering (NRPS) technique<sup>1</sup> is effective in measuring molecular orientation of adsorbed molecules on graphite basal planes. Thus the tilt angles of adsorbed molecules on this surface, such as N<sub>2</sub> and N<sub>2</sub>O, were studied in detail as a function of coverage and temperature.<sup>2,3</sup> In the case of the N<sub>2</sub>-graphite system, our results agree nicely with theoretical calculations which used molecular dynamic simulations.<sup>4,5</sup> The tilt angles of intercalated N<sub>2</sub> molecules in C<sub>24</sub>K and C<sub>24</sub>Rb were also studied.<sup>6,7</sup>

The purpose of the present work is to determine the chemical form of the adsorbed NO<sub>2</sub> molecules, namely, to find out whether it is adsorbed in a monomer or dimer form and also to determine the tilt angle of the molecules with respect to the graphite basal planes. In the NRPS technique,<sup>1</sup> a beam of monoenergetic photons generated from the  $(n, \gamma)$  reaction using thermal neutrons photoexcites the 6324-keV level in <sup>15</sup>N nuclei. Both the incident  $\gamma$  line and the nuclear resonance level are Doppler broadened. The scattered intensity depends on the extent of overlap between the two Doppler-broadened lines. The Doppler width is  $\Delta = E(2kT_e/Mc^2)^{1/2}$ , where  $E$  is the nuclear level energy,  $M$  is the nuclear mass, and  $T_e$  is the effective temperature of the scattering atom; it is related to the *total* kinetic energy of the atom in the sense that it contains the part associated with its internal zero-point motion. Thus the Doppler broadening of the nuclear level depends on the zero-point vibrational motion of the N atom. This makes it possible to use it for studying the directional properties of the normal vibrational modes of the N-containing molecules, and for studying the tilt angles of adsorbed molecules relative to the graphite planes.

The adsorption of NO<sub>2</sub> on the graphite basal plane was studied previously at 90 K, by Sjovald *et al.*<sup>8</sup> They used high-resolution electron-energy-loss spectroscopy (HREELS) and thermal desorption spectroscopy (TDS). They concluded that the NO<sub>2</sub> molecules are adsorbed as dimers and their results

were consistent with the dimers adsorbed with the molecular axis normal to the graphite basal planes. Sjovald *et al.* used a sample of highly oriented pyrolytic graphite (HOPG) with a total surface area of 19×8 mm<sup>2</sup>. In our work, however, we employed a different substrate consisting of 80 g of Grafoil (with specific surface area of about 20 m<sup>2</sup>/g) and used an entirely different method. It is interesting to obtain similar results for the tilt angle of the N<sub>2</sub>O<sub>4</sub> molecules on the graphite, in spite of the different substrates in the two techniques.

### II. THEORETICAL METHOD

#### A. Resonance scattering cross section

As mentioned above, the resonance photon scattering process is caused by a Doppler-broadened  $\gamma$  line [ $F(E)$ , represented by a Gaussian] overlapping by chance a Doppler broadened nuclear level at 6324 keV in <sup>15</sup>N [represented by a  $\psi$  function,  $\psi(x, t)$ , defined below]. This overlap is illustrated schematically in Fig. 1 where the lines are known<sup>1</sup> to be separated by  $\delta=29.5$  eV from each other.

The resonance scattering cross section for such a process and for an infinitely thin <sup>15</sup>N sample is given by the overlap integral which is shown as the shaded area in Fig. 1. This is expressed as

$$\sigma_r = \sigma_0 \int_0^\infty F(E) \psi(x, t) dE = \sigma_0 \psi_0(x_0, t_0), \quad (1)$$

where  $\sigma_0 = 2\pi\lambda^2 g \Gamma_0 / \Gamma$  is the peak cross section of a non-broadened nuclear level whose total natural width is  $\Gamma$  and ground-state width  $\Gamma_0$ . The Gaussian function  $F(E)$  is given by

$$F(E) = (1/\Delta_s \pi^{1/2}) \exp[-(E - E_r + \delta)^2 / \Delta_s^2], \quad (2)$$

where  $\Delta_s$  is the Doppler width of the incident  $\gamma$  line and is defined by

$$\Delta_s = E_s (2kT_s / M_s c^2)^{1/2}. \quad (3)$$

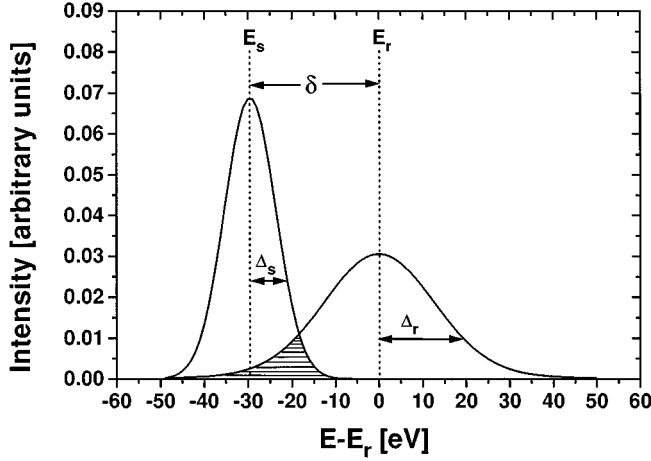


FIG. 1. Calculated shapes of the Doppler-broadened  $\gamma$  line [emitted by the  $^{52}\text{Cr}(n, \gamma)$  reaction] and the nuclear level in  $^{15}\text{N}$ . The former is represented by a Gaussian and the latter by a  $\psi$  function. The overlap integral shown as the shaded area represents the resonance scattering cross section.

$E_s = E_r + \delta$  is the peak energy of the  $\gamma$  line emitted by the  $^{52}\text{Cr}(n, \gamma)$  reaction; it is separated by an energy  $\delta$  from the resonance energy  $E_r$  of the nuclear level (after recoil correction).

In this resonance scattering process, free recoil of the emitting nucleus is assumed; the recoil energy is  $E_R = E_r^2/2Mc^2 = 1.43$  keV and is far larger than the lattice energies of the sample.  $M_s$  is the mass of the emitting isotope of the  $\gamma$  source;  $T_s$  is the effective temperature of Cr defined by Lamb.<sup>9</sup> The function  $\psi(x, t)$  is a convolution between a Breit-Wigner resonance form and a Gaussian distribution of energies and is defined by

$$\psi(x, t) = \left( \frac{1}{2\sqrt{\pi t}} \right) \int_{-\infty}^{\infty} \frac{\exp[-(x-z)^2/4t]}{1+z^2} dz, \quad (4)$$

with

$$x = \frac{2|E - E_r|}{\Gamma}, \quad t = (\Delta_r/\Gamma)^2, \quad (5)$$

$$\Delta_r = E_r(2kT_r/M_r c^2)^{1/2},$$

where  $E_r$ ,  $M_r$ , and  $\Delta_r$  are related to the scatterer and are defined in a similar manner to that of the  $\gamma$  source. The right-hand side of Eq. (1) shows that the overlap integral could be expressed as another  $\psi$  function where

$$x_0 = 2|E_r - E_s|/\Gamma = 2\delta/\Gamma \quad \text{and} \quad t_0 = (\Delta_s^2 + \Delta_r^2)/\Gamma. \quad (6)$$

Thus the scattering cross section depends strongly on the effective temperatures  $T_s$  and  $T_r$  through the corresponding Doppler widths. Since the same  $\gamma$  source was used throughout the entire experiment, we will be interested only in the dependence of  $\sigma_r$  on the effective temperature  $T_r$  of the scatterer which occurs in the form of NO<sub>2</sub> either pure, dimerized, or adsorbed on graphite.

Equation (1) can also be viewed as yielding the scattering intensity for an infinitely thin  $^{15}\text{N}$  target. For a thick sample, one has to account for the atomic and nuclear absorption of

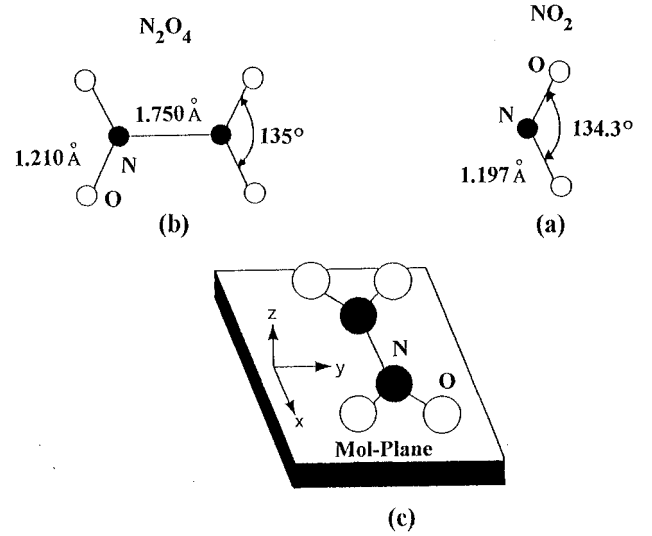


FIG. 2. Geometry of (a) the NO<sub>2</sub> molecule and (b) the N<sub>2</sub>O<sub>4</sub> molecule taken from Ref. 11. (c) The intrinsic  $x$ ,  $y$  and  $z$  axes of the N<sub>2</sub>O<sub>4</sub> molecule.

the incident  $\gamma$  line and for the atomic absorption of the scattered photons. This was done in detail elsewhere.<sup>10</sup> In practice the scattered intensities were calculated using numerical integrations by employing a computer code.

It should be noted that the Doppler width of the incident 6324-keV  $\gamma$  line emitted by the  $^{52}\text{Cr}(n, \gamma)$  reaction is  $\Delta_s = 8.2$  eV (assuming a thermodynamic temperature of 460 K for the  $\gamma$  source), whereas for the 6324-keV resonance level in the  $^{15}\text{N}$  atom in the form of N<sub>2</sub>O<sub>4</sub> (at 296 K),  $\Delta_r = 18.2$  eV. This large difference in the Doppler broadenings is not only due to the different masses and thermodynamic temperatures of the photon source and the scatterer, but mainly due to the different *effective* temperatures being  $T_s = 475$  K and  $T_r = 674$  K of the Cr atom and the N atom, respectively.

## B. Effective temperatures

From the above, it is clear that a calculation of the scattering intensity from the sample requires a knowledge of the effective temperature  $T_e$  of the N atom. We hereby calculate the effective temperatures of the  $^{15}\text{N}$  atom in NO<sub>2</sub> in the various forms encountered in the present work.

### 1. Pure NO<sub>2</sub>

We first note that the NO<sub>2</sub> is a V-shaped molecule whose geometry is described in Fig. 2(a); it performs translational, rotational, and three internal vibrational modes. The effective temperature expresses the total kinetic energy of the N atom including that of its zero-point motion. Thus  $T_e$  of the N atom at a temperature  $T$  may be written as

$$T_e = S_t T_t + S_r T_r + \sum_1^3 S_j k \alpha_j / 3, \quad (7)$$

where the first two terms on the right-hand side are contributed by the external kinetic degrees of freedom of the molecule (with  $S_t$  and  $S_r$  the energy fractions shared by the N atom in the translational and the rotational motions of the entire molecule);  $T_t$  is the effective temperature of the trans-

TABLE I. Calculated fractions  $S_t$ ,  $S_r$ , and  $S_j$  of the intramolecular vibrational, librational, and intermolecular vibrational motions of  $\text{NO}_2$  and  $\text{N}_2\text{O}_4$  molecules. The normal modes of vibration  $\nu_j$  (in  $K$  units) were taken from Ref. 11. The values of the force constants (in units of  $10^5$  dyn/cm) are listed. The calculated values are normalized so that  $S_t + S_r + \sum_1^{12} S_j/3 = 1$ .  $k_{\text{N}=\text{N}} = 2.92$ , stretching force of the N=N bond.  $k_{\text{N}-\text{O}} = 9.34$ , stretching forces of the N—O bonds.  $k_{\text{O}-\text{O}(y)} = 1.25$ , stretching forces of the O—O bonds along the  $y$  direction.  $k_{\text{O}-\text{O}(x)} = 0.20$ , stretching forces of the O—O bonds along the  $x$  direction. Bending force stabilizing the O—N—O angles, equal to 1.113. Bending force stabilizing the O—N=N angles, equal to 0.316. Restoring force of the out-of-plane  $B_{2g}$  mode, equal to 0.003. Restoring force of the out-of-plane  $B_{1u}$  mode, equal to 0.507. Restoring force of the out-of-plane  $A_u$  mode, equal to 0.051.

$j$	$\text{NO}_2$				$\text{N}_2\text{O}_4$			
	$\nu_j$	$S_j$	$S_t$	$S_r$	$\nu_j$	$S_j$	$S_t$	$S_r$
1	2273	0.6444	0.3192	0.2391	1946.6	0.275 16	0.1596	0.0454
2	1878.8	0.1446			1794.7	0.138 62		
3	1064.6	0.5361			1288.1	0.176 87		
4					1046.3	0.201 81		
5					568.8	0.047 96		
6					2448.1	0.334 93		
7					2407.9	0.322 83		
8					392	0.112 29		
9					368.7	0.017 59		
10					939.2	0.416 52		
11					639.4	0.340 41		
12					138.4	0.000 01		

lational and rotational motions of the molecules. The third term corresponds to the internal vibrations of  $\text{NO}_2$ , which has three normal modes: symmetric and antisymmetric stretching of the N—O bonds, and a bending of the O—N—O angle. The corresponding frequencies were taken from Ref. 11 and are listed in Table I, with  $S_j$  the energy fraction of the N atom in the  $j$ th vibrational mode of the molecule. The kinetic part of the vibrational energy  $k\alpha_j$  is given by

$$k\alpha_j/2 = (h\nu_j/2) \{ [\exp(h\nu_j/kT) - 1]^{-1} + \frac{1}{2} \}, \quad (8)$$

where the factor  $\frac{1}{2}$  appearing in  $k\alpha_j$  and  $h\nu_j$  arises from the fact that only the kinetic part of the vibrational energy contributes to the effective temperature and hence to the Doppler broadening of the nuclear level. The fractions  $S_j$  are the ratios of the vibrational energy of the N atom and that of the three atoms of the molecule:

$$S_j = 4\pi\nu_j^2 M_i A_{ij}^2 / \left( 4\pi\nu_j^2 \sum_1^3 M_i A_{ij}^2 \right), \quad (9)$$

with  $A_{ij}$  the amplitude of atom  $i$  in the vibrational mode  $j$  of the V-shaped molecule. The values of  $A_{ij}$  were calculated using the published distances, the O—N—O bond angle, and a rough knowledge of the spring constants governing the vibrational motion of the molecule. Using the values of  $S_t$ ,  $S_r$ , and  $S_j$  obtained from the above procedure (listed in Table I), we obtain

$$T_e = 0.5583T + 384.9. \quad (10)$$

At  $T=300$  K,  $T_e=552$  K where 384.9 K is the zero-point energy of the  $^{15}\text{N}$  atom (in  $\text{NO}_2$ ) and is contributed by the internal vibrational motion.

This expression for  $T_e$  applies to the case of a gaseous  $\text{NO}_2$  sample. For liquid and solid samples,  $T_e$  increases enormously. The increment is contributed by the dimerization of  $\text{NO}_2$  and by the strong interaction between the dimer molecules. To evaluate  $T_e$  for this more complicated case, we first deal with gaseous  $\text{N}_2\text{O}_4$ .

## 2. Pure $\text{N}_2\text{O}_4$

This is a planar molecule whose geometry is described in Fig. 2(b). The effective temperature of the N atom in molecular  $\text{N}_2\text{O}_4$  (in a gaseous form) may be written in a similar fashion to that of Eq. (7). Here, however, one has to account for the 12 vibrational normal modes of the molecule as was done in Ref. 12. The result is

$$T_e = S_t T + S_r T + \sum_1^{12} S_j k\alpha_j/3. \quad (11)$$

After substituting the calculated  $S_j$  (see Table I), we obtain, for a gaseous  $\text{N}_2\text{O}_4$ ,

$$T_e = 0.205T + 585.1. \quad (12)$$

Here, 585.1 K represents the contribution of the zero-point motion of the N atom in  $\text{N}_2\text{O}_4$  to  $T_e$  and is much larger than the corresponding value in a  $\text{NO}_2$  monomer. The different values of  $T_e$  for a monomer and a dimer as revealed in Eqs. (10) and (12) has two consequences. First, the scattered  $\gamma$ -ray intensity from  $^{15}\text{N}$  (which is proportional to  $T_e$ ) in the form of a dimer is much stronger than that from a monomer. Second, the variation of  $T_e$  with  $T$  is also different for the two cases. Thus, by measuring the scattered  $\gamma$ -ray intensity from a sample and its variation with  $T$ , it is very easy to decide in what form the N atom occurs in that sample.

It will be necessary to calculate  $T_e$  of the N atom along the three intrinsic coordinate axes of the N<sub>2</sub>O<sub>4</sub> molecule as shown in Fig. 2(c) which we denote by  $T_x$ ,  $T_y$ , and  $T_z$ . This is done by projecting the translational, rotational, and vibrational motion (of each normal mode) of the molecule along the above three directions. The results for a free dimer assumed to be in a gaseous phase are

$$T_x = S_x T_t + \sum_1^5 S_j \alpha_j, \quad T_y = S_y T_t + \sum_6^9 S_j \alpha_j, \\ T_z = S_z T_t + \sum_{10}^{12} S_j \alpha_j, \quad (13)$$

with  $S_x=0.1596$ ,  $S_y=0.2125$ ,  $S_z=0.2431$ , where  $S_x$ ,  $S_y$ , and  $S_z$  are the energy fractions of the translational and rotational motions of the N atom along the three coordinate axes of the molecule.

### 3. N<sub>2</sub>O<sub>4</sub> adsorbed on fully oriented graphite

There is a small difference between the  $T_e$  for a N<sub>2</sub>O<sub>4</sub> molecule in a gaseous form and in an adsorbed form. The increment is due to the binding effects of the dimer-dimer and dimer-graphite interactions. In order to compare our measured scattering intensities with calculations, we have to define two effective temperatures of the <sup>15</sup>N atom:  $T_{\parallel}$  and  $T_{\perp}$  in directions parallel and perpendicular to the graphite planes.  $T_{\parallel}$  and  $T_{\perp}$  may be evaluated by making the following assumptions. (1) The in-plane and out-of-plane degrees of freedom of the motion of the N<sub>2</sub>O<sub>4</sub> molecule with respect to the graphite surface are decoupled. (2) The adsorption process has no influence on the internal vibrational frequencies and on the geometry of the molecule. (3) The relative motion of the N<sub>2</sub>O<sub>4</sub>-graphite system can be represented by six Einstein oscillators: (i) an out-of-plane vibration of the entire dimer with respect to the graphite plane, (ii) an out-of-plane libration and two in-plane librations, and (iii) two in-plane degenerate vibrations of the entire dimer. Here we simplify matters by choosing a single effective frequency  $\nu_1$  for the four in-plane motions and another,  $\nu_2$ , for the two out-of-plane motions. Furthermore, we may take  $\nu_1 = \nu_2$ , and justify this choice by noting that the in-plane intermolecular interaction is expected to be weaker than that in solid N<sub>2</sub>O<sub>4</sub> due to the large average distance between the adsorbed dimers (where a submonolayer coverage of N<sub>2</sub>O<sub>4</sub> on Grafoil was employed in the present work).

It should be noted in this connection that the N<sub>2</sub>O<sub>4</sub>-graphite interaction is known to be much weaker than that between the N<sub>2</sub>O<sub>4</sub> molecules. In fact, the Debye temperature of solid N<sub>2</sub>O<sub>4</sub> (which is a measure of the intermolecular interactions) was measured<sup>12</sup> and found to be 315 K. However, the N<sub>2</sub>O<sub>4</sub>-Grafoil interaction, expressed as an effective temperature and deduced from the temperature variation of the scattering intensity off the N<sub>2</sub>O<sub>4</sub>-Grafoil sample, is around 200 K (see Fig. 3 and Sec. IV B below).

With the above assumptions, we may write the expressions of  $T_{\parallel}$  and  $T_{\perp}$  for the following three orientations of the N<sub>2</sub>O<sub>4</sub> plane with respect to the  $G$  surface (see Fig. 4): (a) N<sub>2</sub>O<sub>4</sub> plane parallel ( $\theta=0^\circ$ ) to the  $G$  surface, (b) N<sub>2</sub>O<sub>4</sub> plane normal to the  $G$  surface ( $\theta=90^\circ$ ), with the N=N bond nor-

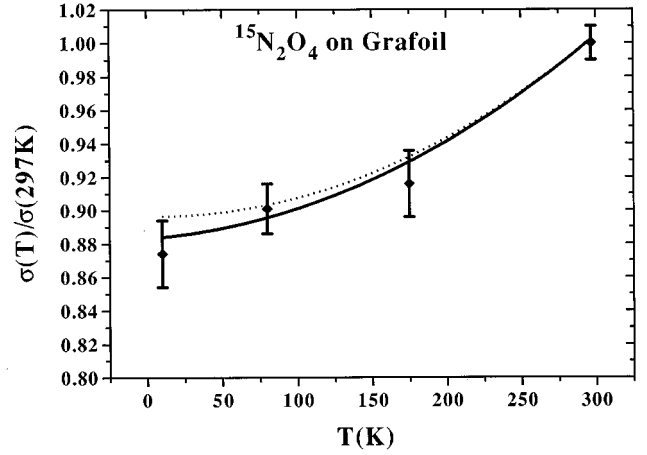


FIG. 3. Scattered intensity ratios (relative to 297 K) from the NO<sub>2</sub>-Grafoil sample contained in a 5×5 cm<sup>2</sup> stainless steel cylinder. The Grafoil weight is 80 g in which 823 mg gas was adsorbed. The effective temperature of the  $\gamma$  source is 475 K. The solid curves were calculated after deducing the effective temperatures and  $\sigma_r$  of the N atom in the N<sub>2</sub>O<sub>4</sub>-Grafoil system. The “effective” Debye temperature  $\Theta$  was then deduced by best fitting the solid curves to the experimental data. Typical errors are indicated.

mal to it, (c) N<sub>2</sub>O<sub>4</sub> plane stands on the  $G$  surface ( $\theta=90^\circ$ ), with the N=N bond parallel to it. The results are given in Table II.

The above equations may be used for calculating the effective temperature  $T_g$  for *non-oriented* graphite using the relation

$$T_g = (2T_{\parallel} + T_{\perp})/3. \quad (14)$$

It is interesting to note that the same value is obtained no matter which pair of values of  $T_{\parallel}$  and  $T_{\perp}$  (see Table II) is used for calculating  $T_g$  of Eq. (14). This result is intuitively expected and is viewed as a self-consistency check of the formula given in Table II.

### 4. N<sub>2</sub>O<sub>4</sub> adsorbed on Grafoil

The above values of  $T_{\parallel}$  and  $T_{\perp}$  (Table II) are valid for the *fully oriented* graphite surface. In practice, one has to account for the actual structure of the adsorbing surface (Grafoil) which consists of a randomly oriented fraction ( $f=0.44$ ) of crystalline surfaces having a mosaic spread with a full width at half maximum (FWHM) angle  $\phi=30^\circ$ . The corrected values,  $T_{\parallel}^c$  and  $T_{\perp}^c$ , may be written as

$$T_{\perp}^c = fT_g + (1-f)\{T_{\perp}\langle\cos^2\varphi\rangle + T_{\parallel}\langle\sin^2\varphi\rangle\}, \quad (15)$$

$$T_{\parallel}^c = (3T_g - T_{\perp}^c)/2. \quad (16)$$

The corrected values  $T_{\parallel}^c$  and  $T_{\perp}^c$  were calculated as a function of  $T$  for each of the N<sub>2</sub>O<sub>4</sub> orientations relative to the  $G$  surface (see Fig. 4). The corresponding scattering cross sections may be obtained using the solid curve of Fig. 5 from which the values of  $R = \sigma_{\parallel}/\sigma_{\perp}$  as a function of  $T$  were deduced and are displayed in Fig. 4.

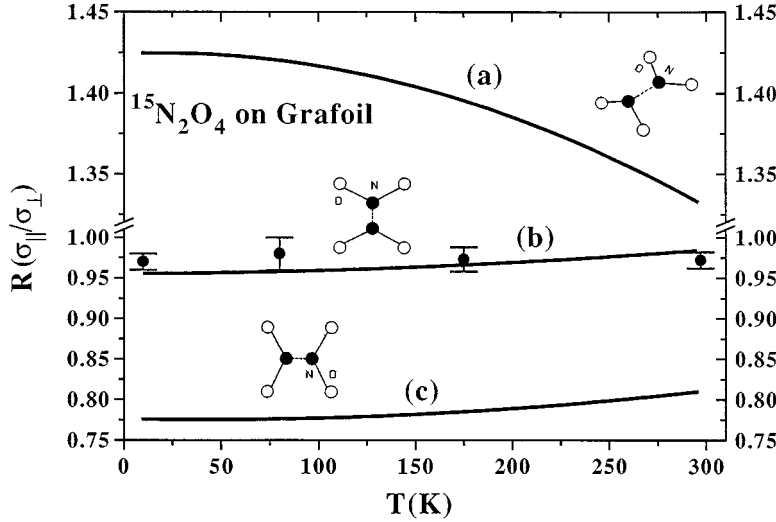


FIG. 4. Measured and calculated scattered intensity ratios  $R(\sigma_{||}/\sigma_{\perp})$  with the photon beam parallel and normal to the  $G$  planes for the following cases. (a) The molecular plane is assumed parallel to the  $G$  planes. (b) The molecule is assumed to be standing on the  $G$  plane with its axis normal to it. (c) A standing  $N_2O_4$  molecule with its symmetry axis parallel to the  $G$  plane.

### III. EXPERIMENTAL DETAILS

#### A. $NO_2$ adsorption measurements

Our first task in this adsorption study was to find out whether the  $NO_2$  molecules form a genuine monolayer film on the graphite (0001) basal plane. The substance chosen for our study was the well-known exfoliated graphite, namely, Grafoil. We used a 1.729-g sheet of Grafoil to perform a vapor-pressure isotherm measurement at 273 K, keeping in mind that at 273 K, nitrogen dioxide is known to be mostly in a dimer form.

The usual procedure is to heat the Grafoil under vacuum ( $P=10^{-6}$  torr) to 950 °C for 4 h in order to desorb the surface impurities. When cold, the Grafoil is transferred to a cell in helium atmosphere in a sealed plastic bag. The cell, equipped with a valve, is connected to the adsorption system containing a calibrated volume and a Baratron pressure gauge. The “dead” volume of the cell is then measured by recording the pressure as a function of the calibrated He volumes introduced into the adsorption cell.

This procedure could be used because no He adsorption takes place at room temperature. The specific adsorption area of Grafoil was found to be 20 m<sup>2</sup>/g; it was deduced by measuring the isothermal adsorption of  $N_2$  at liquid nitrogen temperature. The isothermal adsorption of  $NO_2$  was then determined by measuring the adsorbed volume  $V_{ads}$  versus the pressure  $P/P_0$ . The data, displayed in Fig. 6, reveal a “knee” characteristic of the completion of the first atomic

layer. The results were analyzed, using the Brunauer-Emmett-Teller (BET) model,<sup>13,14</sup> to determine the surface area occupied by a single  $N_2O_4$  molecule yielding 16.4 Å<sup>2</sup>.

This should be compared with the corresponding area occupied by a single  $N_2$  molecule, which is 16 Å<sup>2</sup>. The latter result may be viewed as independent evidence that the  $N_2O_4$  does not lie flat on the  $G$  surface because a lying  $N_2O_4$  molecule occupies an estimated surface area of around 29 Å<sup>2</sup>. In fact, the surface area of a standing  $N_2O_4$  molecule with its N=N axis parallel to the  $G$  surface is larger than that with its N=N axis normal to the  $G$  surface. The surface area of the latter orientation is in better agreement with the measured result and therefore favors the normal geometry of the N=N axis with respect to the  $G$  surface.

#### B. Photon scattering measurements

For the photon scattering measurements, we used a large Grafoil sample (80 g) consisting of about 100 rectangular sheets, each 0.5 mm thick, of varying dimensions packed parallel to each other. It was inserted into a thin-walled 5×4.8 cm<sup>2</sup> cylindrical stainless steel cell fitted by a valve. The Grafoil sheets were arranged with their long axis parallel to that of the cylindrical container and with their  $c$  axes normal to it and along one radius of the cylinder. Isotopic  $NO_2$  (99% <sup>15</sup>N) was allowed into the Grafoil cell; the amount

TABLE II. Expressions for the effective temperatures  $T_{||}$  and  $T_{\perp}$  of the N atom along and normal to the Grafoil planes for various configurations of the  $N_2O_4$  molecule with respect to the Grafoil planes.

Configuration	$T_{  }$	$T_{\perp}$
Molecular plane $\parallel$ to $G$ plane	$(T_x + T_y)/2$	$T_z = S_z T_i + \sum_{j=10}^{12} S_j \alpha_j$
Molecular axis $\parallel$ to $G$ plane (standing molecule)	$(T_x + T_z)/2$	$T_y = S_y T_i + \sum_{j=6}^9 S_j \alpha_j$
Molecular axis $\perp$ to $G$ plane (standing molecule)	$(T_y + T_z)/2$	$T_x = S_x T_i + \sum_{j=1}^5 S_j \alpha_j$

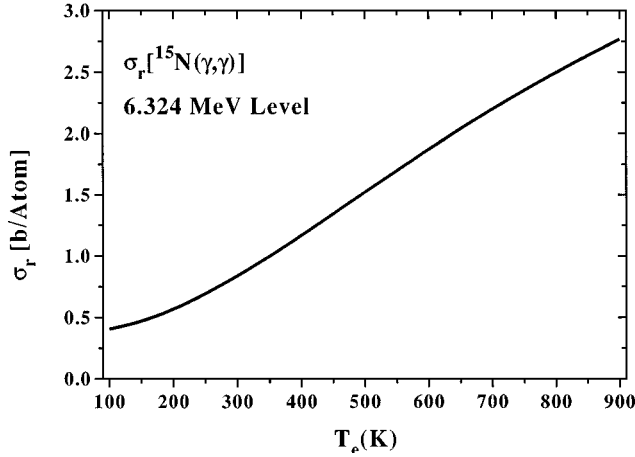


FIG. 5. Resonance scattering cross section  $\sigma_r$  of the 6324-keV line [emitted by the  $^{52}\text{Cr}(n,\gamma)$  reaction] versus the effective temperature  $T_e$  of  $^{15}\text{N}$  for a  $\gamma$ -source effective temperature  $T_s=475$  K. The parameters of the resonance scattering process which we used in the calculations are  $\Gamma=\Gamma_0=2.9$  eV (where  $\Gamma$  and  $\Gamma_0$  are the total and ground-state radiative widths of the 6324-keV level in  $^{15}\text{N}$ );  $\delta=29.5$  eV is the energy difference between the peaks of the incident  $\gamma$  line and the  $^{15}\text{N}$  nuclear level (after recoil correction). The Debye temperature of the Cr  $\gamma$  source was taken to be 473 K (Ref. 15).

of gas corresponded to a coverage of less than one monolayer. This choice of gas coverage was made to avoid any density compression of the gas film, as we expected the tilt angle of the gas to change with increasing coverage. The Grafoil cell was placed inside a variable temperature (297 to 12 K) cryostat whose axis coincided with the geometrical axis of the sample and could be rotated from a position where the photon beam was parallel to the  $c$  axis of the sample to a perpendicular geometry and vice versa. The background radiation spectrum was measured using an identical stainless steel cylinder containing nonoriented graphite, with the same weight and similar geometry as that of the Grafoil sample.

The photon source in the present work was generated from the  $(n,\gamma)$  reaction on disks of metallic chromium placed along a tangential beam tube and near the core of the IRR-2 (Israel Research Reactor-2). A total of four disks of Cr was used, each having a diameter of 8 cm and thickness of 1.5 cm. The photon beam thus obtained was collimated and neutron filtered by passing it through a 40-cm-long borated paraffin before hitting the sample. The resulting intensity of the 6324-keV line was about  $10^4$  photons/cm<sup>2</sup>s on the sample position.

For detecting the scattered radiation, two hyperpure Germanium (HPGe) detectors with efficiencies of 35% and 30% were used, set at scattering angles of 115° and 130° and distances of 20 cm from the geometrical center of the target. The detectors were protected against the background of fast neutrons by covering them with a 1-cm shield of borated plastic. The intense low-energy scattered photons from the sample were reduced using a photon hardener consisting of around 1 cm of lead. The  $\gamma$ -ray resolution of the system was around 9 keV at 6324 keV. Other experimental details of the system are described elsewhere.<sup>1,10</sup>

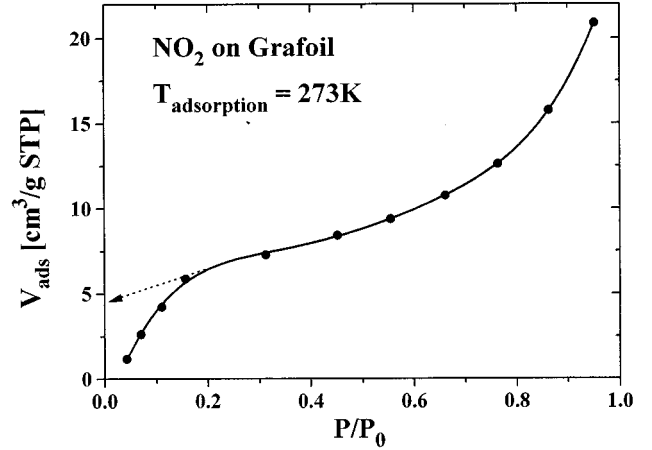


FIG. 6. Vapor-pressure isotherm at 273 K for NO<sub>2</sub> adsorbed on a 1.73-g Grafoil sample contained in a 14-cm<sup>3</sup> stainless steel cylinder. The adsorbed volume of NO<sub>2</sub> was corrected for the dead volume of the Grafoil cell. The amount of NO<sub>2</sub> corresponding to a monolayer completion is indicated.

## IV. RESULTS AND DISCUSSION

### A. Nature of the adsorbed NO<sub>2</sub>

From the expressions of  $T_e$  given in Eqs. (10) and (12), it is clear that the predicted scattering cross sections from  $^{15}\text{N}$  in a monomer (NO<sub>2</sub>) form is markedly smaller than that of a dimer (N<sub>2</sub>O<sub>4</sub>) form. This fact was used for identifying the adsorbed species of NO<sub>2</sub> on Grafoil. To do this, we used as a reference a sample of ammonia ( $^{15}\text{NH}_3$ ) adsorbed on Grafoil (at 90 K); its scattering intensity was then compared with that of NO<sub>2</sub>-Grafoil (at 296 K) contained in identical cells with the same amounts of  $^{15}\text{N}$  and Grafoil. The effective temperatures<sup>15</sup> for the above two samples are predicted to be 460 and 674 K (for dimer adsorption), respectively, leading to scattering cross sections:  $\sigma_r(\text{NH}_3)=1.38$  b and  $\sigma_r(\text{N}_2\text{O}_4)=2.12$  b whose ratio is 1.54. For monomer adsorption, the predicted ratio is 1.02 because  $T_e(\text{NO}_2)=463$  K. Those predicted ratios should be compared with a measured cross section ratio:  $R_{\text{expt}}=1.50\pm 0.06$ . This shows that at room temperature, the NO<sub>2</sub> is adsorbed primarily in a dimer form and not as a monomer.

### B. Temperature effect of the NO<sub>2</sub>-Grafoil system

The resonance scattering intensity  $\sigma_r$  versus  $T$  for  $^{15}\text{NO}_2$  adsorbed on Grafoil was measured; the results are displayed in Fig. 3, which also shows previous data for pure  $^{15}\text{NO}_2$  taken from Ref. 12. Both data were taken at a  $\gamma$ -source effective temperature,  $T_s=475$  K. Note that the  $\sigma_r$  decreases faster with  $T$  than pure NO<sub>2</sub>, which means that the NO<sub>2</sub>-graphite binding is much weaker than that of the pure molecules. Such data may be used for estimating the binding properties of the NO<sub>2</sub>-graphite system by applying the assumptions made in Sec. III B. In the latter case of pure N<sub>2</sub>O<sub>4</sub>, the Debye temperature was deduced<sup>12</sup> and found to be  $\Theta=315$  K. In a similar manner, the results of Fig. 3 were used for deducing an “effective” Debye temperature for the N atom in the NO<sub>2</sub>-graphite system. The results are consistent with  $\Theta\approx 200$  K, and much lower than that of pure N<sub>2</sub>O<sub>4</sub>.

This indicates that the  $N_2O_4$ -graphite interaction potential is much weaker than the intermolecular potential in pure  $N_2O_4$ .

### C. Tilt angle of adsorbed $N_2O_4$

The ratio  $R = \sigma_{\parallel} / \sigma_{\perp}$  of scattered intensities from the  $NO_2$ -Grafoil system with the beam parallel and normal to the graphite planes was measured at 12, 80, 175, and 296 K. The measured data, together with the values calculated for the three geometries, are shown in Fig. 4. It may be seen that our data are in very good agreement with the calculated values where the  $N_2O_4$  molecule stands on the Grafoil surface with its N=N bond normal to the planes and that a huge departure exists from the other two geometries. It also shows that this tilt angle is essentially the same throughout the entire temperature range between 12 and 296 K. From the measured error margin of the data shown in Fig. 4, we estimated the corresponding uncertainty in the tilt angle of the  $N_2O_4$  molecule; the result is  $90^{\circ} \pm 6^{\circ}$ . The result of Sjovald *et al.*<sup>8</sup> carried out at 90 K and using the HREELS technique is consistent with that obtained in the present work.

### D. Comparison with other systems

It is of interest to compare the tilt measured in the present work with similar studies on adsorption and intercalated systems.<sup>16</sup> For adsorbed gases such as  $N_2$  and  $N_2O$  on Grafoil, a similar measurement at 12 K, using the NRPS technique,<sup>2,15</sup> yielded  $\sigma_{\parallel} / \sigma_{\perp} = 1.64$  and 1.32, respectively, which showed that the adsorbed  $N_2$  and  $N_2O$  molecules lay very nearly parallel to the graphite planes and hence the behavior of the latter molecules differs markedly from that of the present work. Furthermore, while the average tilt of the

$N_2$  molecules increased relatively quickly with  $T$ , the tilt of the  $N_2O$  molecules remained almost stable between 12 and 250 K.

In another system, in which the  $HNO_3$  molecules were intercalated into graphite,<sup>17,18</sup> two different situations were observed. In the "normal" compound,<sup>17</sup>  $C_{10}(HNO_3)$ , the  $NO_3$  planar molecule was found to be nearly perpendicular to the graphite hexagonal planes, with a tilt of  $82^{\circ} \pm 8^{\circ}$  while in the "residue" compound,<sup>18</sup>  $C_{15}(HNO_3)$ , which is the more stable species of the former compound, the tilt angle was found to be  $13^{\circ} \pm 5^{\circ}$ . In the last two systems, no variation of the tilt angle with  $T$  below 300 K was observed. Thus the behavior of a standing molecule on graphite, observed in the present system, resembles that of the  $NO_3$  molecules in the "normal" graphite intercalated compound and differs from that of the more stable "residue" compound.

### V. CONCLUSIONS

We have shown that the NRPS technique can be used for the determination of the chemical species of the molecules adsorbed on the graphite surface and we provided firm evidence that the  $NO_2$  is adsorbed on Grafoil in a dimer form and not as a monomer. In addition, we used the same technique to determine the temperature dependence of the tilt angle and the geometry of the dimer molecule with respect to the graphite planes.

### ACKNOWLEDGMENTS

We would like to thank M. Fogel for technical assistance and help in taking the data. This research was supported by the German-Israeli Foundation for Scientific Research and Development (G.I.F.)

<sup>1</sup>R. Moreh, O. Shahal, and V. Volterra, Nucl. Phys. **A262**, 221 (1976).

<sup>2</sup>R. Moreh and O. Shahal, Surf. Sci. **177**, L963 (1986).

<sup>3</sup>R. Moreh and O. Shahal, Phys. Rev. B **40**, 1926 (1994).

<sup>4</sup>A. D. Migone, H. K. Kim, M. H. W. Chan, J. Talbot, D. J. Tildesley, and W. A. Steele, Phys. Rev. Lett. **51**, 192 (1983).

<sup>5</sup>J. Talbot, D. J. Tildesley, and W. A. Steele, Faraday Discuss. Chem. Soc. **80**, 1 (1985).

<sup>6</sup>R. Moreh, S. Melloul, and H. Zabel, Phys. Rev. B **47**, 10 754 (1993).

<sup>7</sup>R. Moreh, H. Pinto, Y. Finkelstein, V. Volterra, and Y. Birenbaum, Phys. Rev. B **52**, 5330 (1995).

<sup>8</sup>P. Sjovald, S. K. So, B. Kasemo, R. Franchy, and W. Wo, Chem. Phys. Lett. **171**, 125 (1990).

<sup>9</sup>W. E. Lamb, Phys. Rev. **55**, 190 (1939).

<sup>10</sup>R. Moreh, S. Shlomo, and A. Wolf, Phys. Rev. C **2**, 1144 (1970).

<sup>11</sup>G. Herzberg, *Infrared and Raman Spectra* (Van Nostrand Reinhold, New York, 1968).

<sup>12</sup>R. Moreh, D. Levant, and E. Kunoff, Phys. Rev. B **45**, 742 (1992).

<sup>13</sup>J. K. Kjems, L. Passell, H. Taub, J. G. Dash, and A. D. Novaco, Phys. Rev. B **13**, 1446 (1976).

<sup>14</sup>D. M. Young and A. D. Crowell, *Physical Adsorption of Gases* (Butterworths, London, 1962).

<sup>15</sup>R. Moreh and O. Shahal, Phys. Rev. B **42**, 913 (1990).

<sup>16</sup>R. Moreh, Appl. Phys. A **51**, 203 (1990).

<sup>17</sup>R. Moreh and O. Shahal, Solid State Commun. **43**, 529 (1982).

<sup>18</sup>R. Moreh, O. Shahal, and G. Kimmel, Phys. Rev. B **33**, 5717 (1986).